NTNU
Kunnskap for en bedre verden

DEPARTMENT OF MATHEMATICAL SCIENCES

TMA4500 - INDUSTRIAL MATHEMATICS, SPECIALIZATION PROJECT

Riemannian Optimization using second order information on the Symplectic Stiefel manifold

Author:
Ole Gunnar Røsholt Hovland

18th December 2024

Abstract

This report explores optimization algorithms on Riemannian manifolds, which are problems where the cost function is defined on a smooth manifold. Riemannian optimization is used in many problems, for example in machine learning, robotics and scientific computing. The report reproduces some results from Jensen and Zimmermann [11] and Bendokat and Zimmermann [3]. In particular we investigate the Riemannian gradient descent method and the Riemannian trust-region method. To compare the algorithms we apply them to multiple optimization problems of symplectic nature, as well as evaluating the impact of different retractions on the algorithms performance. All of the code have been implemented in Julia using the package Manopt.jl [4]. Apart from mostly reaffirming the results in the aforementioned papers, we also find that the pseudo-Riemannian geodesic retraction, introduced by Bendokat and Zimmermann, performs competitively.

Table of Contents

List of Figures

List of Tables

1 Introduction

In this report we will investigate algorithms that perform optimization on Riemannian manifolds. As noted in the preface of [6], because of the inherent structure of some problems, they can be re-described as problems on some smooth manifold. This could be because of of the problem's natural geometry, latent data simplicity, symmetry and/or positivity. Formulating problems through the lens of smooth manifolds has proven successful in the fields of machine learning, computer vision and robotics, signal processing, scientific computing. Optimization on manifolds is a field started around fifty years ago, and has in resent years garnered more attention and recognition. Optimization on Riemannian manifolds, or simply Riemannian optimization, is a field of optimization where, in an effort to optimize some cost function, one restricts the search space to a Riemannian manifold $\mathcal{M}$. Specifically, instead of defining the problem in terms of restrictions on a Euclidean space, one defines the problem on an appropriate Riemannian manifold. The result of this is that we are, in a sense, encoding the restrictions into inherent properties of the search space. To this end one defines the cost function to be a smooth function inherently defined the manifold, $f\colon \mathcal{M} \to \mathbb{R}$. This results in the following, now unconstrained, optimization problem:

$$\min_{p\in\mathcal{M}} f(p). \tag{1.1}$$

To solve this problem we employ optimization algorithms adapted to work inherently on the Riemannian manifold. Many of these algorithms can, among other things, exploit the information contained in the smoothness in the cost function. The algorithm is called a first order algorithm if it only utilizes the gradient of the cost function, or of second order if it also leverages the Hessian, as a means to find the critical point of (1.1) more efficiently. Despite this, in applications, the computational cost of computing the gradient and Hessian can be expensive. This means that, for algorithms using the gradient or Hessian in every iteration, the time to compute each iteration can be higher than that of an algorithm not relying on smoothness information. However, as each iteration could be a better guess, in the sense that the iteration moves us closer to the critical point, the total number of iterations are usually lower for higher order algorithms. For some problems the number of iterations is so low as to compensate for the higher computational cost per iteration, while for other problems the less accurate but faster lower order algorithms are the optimal choice.

The main goal of this project report is to reproduce some of the findings, programmed in the programming language MATLAB, of Jensen and Zimmermann [11] while programming the experiments in the programming language Julia. To this end we investigate the performance of the first order algorithm "gradient descent" and the second order algorithm called the "trust-region method". We apply these algorithms to problems defined on the symplectic Stiefel manifold, where we solve the problem of finding the nearest symplectic matrix to a given non-symplectic matrix. We also investigate the symplectic decomposition problem. The secondary goal of this report is to investigate the performance of different retractions on algorithm performance, investigated by Bendokat and Zimmermann [3]. Provide a partial summary theory outlined in both of these papers, as well as other sources mentioned explicitly throughout the report. Regarding original works, some proofs have been worked out independently by the author of this report. Also, regarding the retraction called pseudo-Riemannian geodesic, investigated in [3], we investigate it further than what was done in the original paper. It will be stated explicitly when something is original work.

The structure of the report is as follows. In Section 2, called "introductory theory", foundational definitions are described, as well as necessary introductions to the symplectic group and the symplectic Stiefel manifold. The foundational definitions is the only part of the report formatted as a reference work, which means that this section consists of disjoint definitions coining the notation used in the report, as well as serving as a refresher to the underlying theory of the rest of the report. Section 3, named "right-invariant framework on the symplectic Stiefel", outlines the theory which is the main contribution of [3], namely arriving at explicit geodesic equations through defining an appropriate right-invariant metric. We then use these results to define the Riemannian gradient and Hessian before finishing the section with some particular results bridging some gaps from the theory to the application. After the theory has been outlined, Section 4, named "Algorithms", introduces the Riemannian gradient descent and the Riemannian trust region method. Lastly the section comments on how the algorithms for the experiments were implemented. Section 5, called "numerical experiments", contains the description and results of the experiments retraction

comparison through the nearest symplectic matrix problem, comparing the performance of the Riemannian gradient descent- and Riemannian trust-region algorithm through the nearest symplectic matrix problem, and finally comparing the aforementioned algorithms through the problem of performing a proper symplectic decomposition. Lastly Section 6, named "conclusion" contains the discussion and conclusion of the report, where we summarize our findings, discuss the results, and suggest directions of further work.

Note that this project report was written in LaTeX, based on the template made by Jon Arnt Kårstad [12].

2   Introductory Theory

In this section we will first cover some foundational definitions in the style of a reference work. We will then proceed with defining the symplectic group, and lastly the symplectic Stiefel manifold. Though the goal of this report is to perform experiments on the symplectic Stiefel manifold, this manifold is interlinked with the symplectic group. Namely, it is a special kind of submanifold, called a quotient manifold, of the symplectic group. After defining necessary concepts on the symplectic group, we will leverage this property to define a right-invariant framework on the symplectic Stiefel manifold. This will enable us to define geodesics, the Riemannian gradient, and ultimately the Riemannian Hessian on the Symplectic Stiefel manifold.

The theory presented in this report is based on the works of Bendokat and Zimmermann [3], and Jensen and Zimmermann [11], with the goal of reproducing some of their findings. Other references will be mentioned as needed, and we will strive to clearly indicate when a section is based on original work.

2.1   Foundational definitions

This section is designed to be a reference work to set notation, and to make the rest of the report more readable in the sense that we do not take detours to define basic properties. Note that even though the elements of the symplectic group and symplectic stiefel manifold are matrices, the word "point" will be used to refer to a specific matrix, as the specific matrix is a point on the matrix manifold.

Definition 1 (Orthogonal group)**.** *The* real Orthogonal group *is defined as the set of all orthogonal matrices in $\mathbb{R}^{n \times n}$, denoted by* O(n)*. [8, p. 3]*

Definition 2 (Quotient manifold)**.** *We define the definition of quotient manifold as in [1, p. 27]. Let $\mathcal{M}$ be a manifold equipped with the operation $\sim$ called the* equivalence relation*. The equivalence relation has the following properties:*

  1. (reflexive) $p \sim p$ for all $p \in \mathcal{M}$,

  2. (symmetric) $p \sim q$ if and only if $q \sim p$ for all $q, p \in \mathcal{M}$, and

  3. (transitive) given $p \sim q$ and $q \sim r$ this implies that $p \sim r$ for all $p, q, r \in \mathcal{M}$.

Given the set $[p] \coloneqq \{q \in \mathcal{M} \colon q \sim p\}$ called the equivalence class *of all points equivalent to p, the set*

$$\mathcal{M}/ \sim \ \coloneqq \{[p] \mid p \in \mathcal{M}\}$$

is called the quotient *of $\mathcal{M}$ by $\sim$. It is the set of all equivalence classes of $\sim$ in $\mathcal{M}$. The mapping $\pi \colon \mathcal{M} \to \mathcal{M}/ \sim$ called the* natural- *or* canonical projection*, defined by $p \mapsto [p]$.*

Definition 3 (Tangent Space)**.** *Following [6, Def. 8.33], for a point p on a smooth manifold $\mathcal{M}$, denote the set of smooth curves [6, Def. 8.5] passing through p at $t = 0$ as C_p. This means that $\alpha(0) = p$ for all $\alpha \in C_p$. For $\alpha, \beta \in C_p$ we say that they are equivalent if*

$$(\phi \circ \alpha)'(0) = (\phi \circ \beta)'(0),$$

meaning their derivatives match in a coordinate chart *(defined as in [14, p. 4]) if their derivatives in the coordinate chart at zero are equal. Denote this equivalence relation as $\alpha \sim \beta$. It has analogous properties to the equivalence relation in Definition 2. The equivalence class is defined as $[\alpha] = \{\beta \in C_p \mid \alpha \sim \beta\}$. Every equivalence class is called a* tangent vector *to $\mathcal{M}$ at p. The* tangent space *at p is the quotient set*

$$T_p\mathcal{M} = C_p / \sim = \{[\alpha] \mid \alpha \in C_p\}.$$

We denote the tangent bundle *as $T\mathcal{M} = \bigsqcup_{p \in \mathcal{M}} T_p\mathcal{M}$, where $\bigsqcup$ denotes the disjoint union.*

Definition 4 (Riemannian manifold)**.** *As defined in [5, def 2.6, p. 179]: a* smooth manifold $\mathcal{M}$, *as defined in [14, p. 13], is a* Riemannian manifold *if we can define a field of symmetric, positive definite, bilinear forms $g(\cdot, \cdot)$, called the* Riemannian metric. *By field we mean that g_p is defined on the tangent space $T_p\mathcal{M}$ at each point $p \in \mathcal{M}$ [5, def 2.1, p. 178]. We will assume that g is smooth, meaning that it is of class $\mathcal{C}^\infty$.*

Definition 5 (Vector field on a Riemannian manifold)**.** *Following Appendix A of [11], a smooth vector field $\mathcal{X}: \mathcal{M} \to T\mathcal{M}$, $p \mapsto \mathcal{X}(p) \in T_p\mathcal{M}$ on a Riemannian manifold $\mathcal{M}$ can be expressed through local coordinates as*

$$\mathcal{X}(p) = \sum_{i=1}^{n} \alpha_i \partial_i =: \boldsymbol{\alpha}^{\mathrm{T}} \boldsymbol{\partial},$$

where $\boldsymbol{\alpha} \in \mathbb{R}^n$, and $\boldsymbol{\partial}$ is the canonical basis of $T_p\mathcal{M}$.

Definition 6 (Whitney sum)**.** *Restricting the definition in [7, p.114] to our scope, for a manifold $\mathcal{M}$ define subsets of the tangent bundle (see Definition 3) $\mathcal{X}, \mathcal{Y} \subseteq T\mathcal{M}$. The Whitney sum is defined as*

$$\mathcal{X} \oplus \mathcal{Y} \coloneqq \bigsqcup_{p \in \mathcal{M}} \mathcal{X}_p \times \mathcal{Y}_p,$$

where $\bigsqcup$ denotes the disjoint union.

Definition 7 (Horizontal & Vertical Space)**.** *Using Definition 2, given a Riemannian manifold $\overline{\mathcal{M}}$ with Riemannian metric $\overline{g}$, denote a quotient manifold of $\overline{\mathcal{M}}$ as $\mathcal{M} = \overline{\mathcal{M}}/\sim$. Following the definitions in Absil et al. [1, p. 43], for a point $p \in \mathcal{M}$, the equivalence class $[p] = \pi^{-1}(p)$ induces an embedded submanifold of $\overline{\mathcal{M}}$ (see Definition 2), hence it admits a tangent space,*

$$\mathcal{V}_{\overline{p}} = T_{\overline{p}}(\pi^{-1}(p)) = \ker(\mathrm{D}\,\pi(p))$$

[11, p. 4] named the vertical space *at $\overline{p}$. Canonically chosen as the orthogonal complement of $\mathcal{V}_{\overline{p}}$ in $T_{\overline{p}}\overline{\mathcal{M}}$, the* horizontal space *[1, p. 48] is defined as*

$$\mathcal{H}_{\overline{p}} \coloneqq \mathcal{V}_{\overline{p}}^{\perp} = \{Y_{\overline{p}} \in T_{\overline{p}}\overline{\mathcal{M}} \mid \overline{g}(Y_{\overline{p}}, Z_{\overline{p}}) = 0 \quad \forall \quad Z_{\overline{p}} \in \mathcal{V}_{\overline{p}}\}.$$

The horizontal lift *at $\overline{p} \in \pi^{-1}(p)$ of a tangent vector $X_p \in T_p\mathcal{M}$ is the unique tangent vector $X_{\overline{p}} \in \mathcal{H}_{\overline{p}}$ that satisfies $\mathrm{D}\pi(\overline{p})[X_{\overline{p}}] = X_p$. Note that given the horizontal space on $\overline{\mathcal{M}}$, $\mathcal{H}_{\overline{p}} \oplus \mathcal{V}_{\overline{p}} = T_{\overline{p}}\mathcal{M}$, where $\oplus$ denotes the Whitney sum as in Definition 6.*

Definition 8 (Riemannian connection)**.** *The* Riemanian connection, *also known as the* Levi-Civita connection, *is the unique affine connection which is torsion free, and metric compatible [16, Def. 6.4]. In Appendix A of [11], denoting $\mathfrak{X}(\mathcal{M})$ as the space of smooth vector fields on $\mathcal{M}$, it is defined as the unique $\mathbb{R}$-bilinear smooth map on $\mathcal{M}$ with riemannian metric $\langle \cdot, \cdot \rangle_p$*

$$\nabla: \mathfrak{X}(\mathcal{M}) \times \mathfrak{X}(\mathcal{M}) \to \mathfrak{X}(\mathcal{M}), \quad (X, Y) \mapsto \nabla_X Y,$$

such that the following properties hold. Given $X, Y, Z \in \mathfrak{X}(\mathcal{M})$, and $f \in \mathcal{C}^\infty(M)$, $\nabla_X Y$ has the following properties:

1. *(first argument linearity) $\nabla_{fX} Y = f\nabla_X Y$,*

2. *(Leibnitz) $\nabla_X(fY) = (Xf)Y + f\nabla_X Y$,*

3. *(torsion free) $\nabla_X Y - \nabla_Y X = [X, Y]$, where $[\cdot, \cdot]$ is the Lie bracket [14, p. 186], and*

4. *(metric compatibility)* $Z\langle X, Y\rangle = \langle \nabla_Z X, Y\rangle + \langle X, \nabla_Z Y\rangle$.

Definition 9 (Geodesics)**.** *By [16, Def. 14.1] assume we have a Riemannian manifold $\mathcal{M}$ equipped with an affine connection ∇ (as in Definition 8). A curve $c\colon I \to \mathcal{M}$, where I is an open, closed or half-open interval of $\mathbb{R}$, is a* geodesic *if the covariant derivative (defined in Section 3.4) of $c'(t)$ is zero for all t.*

Definition 10 (Riemannian gradient)**.** *As defined in [6, Def. 3.58], for the Riemannian manifold $\mathcal{M}$, let $f\colon \mathcal{M} \to \mathbb{R}$ be a smooth function. The* Riemannian gradient *of f is the vector field $\operatorname{grad} f$ on $\mathcal{M}$ defined uniquely by for all $(p, X) \in T\mathcal{M}$,*

$$\mathrm{D} f(p)[X] = \langle X, \operatorname{grad} f(p)\rangle_p,$$

where D denotes the differential of f at p meaning $(f \circ c)'(0)$ for som curve $c(t)$ like in Definition 3 [6, Def. 3.34]. The $\langle \cdot, \cdot\rangle_p$ denotes the Riemannian metric at the point p.

Definition 11 (Christoffel symbols)**.** *The method we will employ to completely describe a connection (as defined in Definition 8) locally is to describe them through* Christoffel symbols*. Following the definition in [16, p. 100], let ∇ be an affine connection on $\mathcal{M}$. Denote a coordinate vector field on the coordinate open set $(U, p^1, \ldots, p^n) \subseteq \mathcal{M}$ by $\partial_i := \partial/\partial p^i$ as in [16, Appendix A.3]. In this coordinate frame there exist the numbers called Christoffel symbols, Γ_{ij}^k, defined through the following*

$$\nabla_{\partial_i}\partial_j = \sum_{k=1}^{n} \Gamma_{ij}^k \partial_k =: \mathbf{\Gamma}_{ij}^{\mathrm{T}}\partial.$$

Definition 12 (Retraction)**.** *Following [6, Def. 3.47], a* retraction *on a smooth manifold $\mathcal{M}$ is a smooth map,*

$$\mathcal{R}\colon T\mathcal{M} \to \mathcal{M}, \quad (p, X) \mapsto \mathcal{R}_p(X)$$

such that every curve generated from $c(t) = \mathcal{R}_p(tX)$ satisfies $c(0) = p$ and $\dot{c}(0) = X$. Equivalently the conditions can be stated as in [6, p. 40] without the use of curves. For all $p \in \mathcal{M}$, $\mathcal{R}_p(0) = p$, and $\mathrm{D}\,\mathcal{R}_p(0)\colon T_p\mathcal{M} \to T_p\mathcal{M}$, $\mathrm{D}\,\mathcal{R}_p(0)[X] = X$ is the identify map.

Now that we have defined som foundational definitions to this report, we will proceed with defining the symplectic group and the symplectic Stiefel manifold, the objects of interest in this report. Note that for the rest of this project report we denote $\mathcal{M}$ as being a Riemannian manifold unless stated otherwise.

2.2   The Symplectic group

The real *symplectic group* is the space overarching the symplectic Stiefel manifold. In this section we will therefore define the necessary concepts for this group in preparation for the symplectic Stiefel manifold. Following [3, p. 3], to be able to define the symplectic group we first need some preliminary definitions. Define the *symplectic identity* as the following block matrix,

$$J_{2n} := \begin{bmatrix} 0_n & I_n \\ -I_n & 0_n \end{bmatrix},$$

where I_n denotes the $n \times n$ identity matrix. Note that throughout this report, if it is clear from the context, the subscript for I and J will be omitted for the sake of notational clarity. J_{2n} has some properties we will take advantage of frequently:

$$J_{2n}^{\mathrm{T}} = -J_{2n} = J_{2n}^{-1}. \tag{2.1}$$

The symplectic group is defined as the set of matrices which define the symplectic structure in the following sense. We define the real symplectic group as

$$\mathrm{Sp}(2n) := \{p \in \mathbb{R}^{2n \times 2n} \mid p^+ p = I_{2n}\}, \tag{2.2}$$

where $^+$ is defined as the *symplectic inverse* of any matrix $q \in \mathbb{R}^{2n \times 2k}$ such that

$$q^+ := J_{2k}^{\mathrm{T}} q^{\mathrm{T}} J_{2n}. \tag{2.3}$$

Finding the tangent space of $\mathrm{Sp}(2n)$ follows intuitively from the definition, which we will verify ourselves in the following derivation. Let us first look at the tangent space at the identity. Assume we have a curve $c_I(t) \in \mathrm{Sp}(2n)$, such that $c_I(0) = I$ and $\dot{c}_I(0) := \frac{d}{dt}c_I(t)|_{t=0} = X$. Since $c_I(t)$ is a curve on $\mathrm{Sp}(2n)$, by (2.2) it must satisfy the following condition:

$$c_I(t)^{\mathrm{T}} J_{2n} c_I(t) = J_{2n}. \tag{2.4}$$

Taking the derivative of (2.4) with respect to t at $t = 0$, (2.4) becomes

$$\dot{c}_I(t)^{\mathrm{T}} J c_I(0) + c_I(0)^{\mathrm{T}} J \dot{c}_I(0) = 0. \tag{2.5}$$

Recalling that $c_I(0) = I$, defining $\Omega := \dot{c}_I(0)$, and leveraging the symplectic properties (2.1), (2.5) becomes

$$\Omega^+ = -\Omega.$$

We notice that this definition of the tangent space at the identity is equivalent to the definition of the Lie algebra of $\mathrm{Sp}(2n)$ [3, p. 3]. It is given by

$$\mathfrak{sp}(2n) := T_I \mathrm{Sp}(2n) = \{\Omega \in \mathbb{R}^{2n \times 2n} \mid \Omega^+ = -\Omega\}, \tag{2.6}$$

where Ω is called the Hamiltonian matrix.

Now, for a general $p \in \mathrm{Sp}(2n)$, $c(t) = p c_I(t) \in \mathrm{Sp}(2n)$, where $c(0) = p$. Therefore, by translation, we can define the tangent space of $\mathrm{Sp}(2n)$ at any point p as

$$\begin{aligned} T_p \mathrm{Sp}(2n) &= \{\Omega p \in \mathbb{R}^{2n \times 2n} \mid \Omega \in \mathfrak{sp}(2n)\}, \\ &= \{p\Omega \in \mathbb{R}^{2n \times 2n} \mid \Omega \in \mathfrak{sp}(2n)\}. \end{aligned} \tag{2.7}$$

We will verify that this makes sense by inserting $c := c(t)$ in the condition of (2.2) to get

$$c^{\mathrm{T}} p^{\mathrm{T}} J p c = J.$$

We again take the derivative of to get

$$\Omega^{\mathrm{T}} p^{\mathrm{T}} J p + p^{\mathrm{T}} J p \Omega = 0, \tag{2.8}$$

where we used that $c(0) = 0$, and the definition of Ω. Now, multiplying (2.8) by $J^{\mathrm{T}} p$ from the left, and simplifying we again end up with $\Omega^+ = -\Omega$, verifying our claim.

Now that we have defined the symplectic group, and its components that we will use throughout this report, we will move on to defining the symplectic Stiefel manifold.

2.3   The Symplectic Stiefel manifold

Having defined the symplectic group, we introduce the manifold of interest, the real symplectic Stiefel manifold. It is defined as

$$\mathrm{SpSt}(2n, 2k) := \{p \in \mathbb{R}^{2n \times 2k} \mid p^+ p = I_{2k}\}, \tag{2.9}$$

where p^+ is as in (2.3). Following [3, Prop. 3.1], it is explicitly connected to the symplectic group in the sense that $\mathrm{SpSt}(2n, 2k)$ is diffeomorphic to the following quotient manifold of $\mathrm{Sp}(2n)$:

$$\mathrm{SpSt}(2n, 2k) \cong \mathrm{Sp}(2n)/\mathrm{Sp}(2(n-k)),$$

where the notion of quotient manifold is as in Definition 2. It has dimension $\dim(\mathrm{SpSt}(2n, 2k)) = (2n-2k+1)k$. The following piece of insight can give some further intuition on what the symplectic Stiefel manifold is. We note that the Stiefel manifold is a quotient space, as defined in Definition 2, of the orthogonal group as defined in Definition 1 such that $\mathrm{St}(2n, 2k) = \mathrm{O}(n)/\mathrm{O}(n-k)$.

In a similar manner as for the symplectic group, the expression for the tangent space follows straightforwardly from the definition of $\mathrm{SpSt}(2n, 2k)$. Assume we have a curve, $c(t) \in \mathrm{SpSt}(2n, 2k)$,

such that $c(0) = p$ and $\dot{c}(0) \coloneqq \frac{d}{dt}c(t)|_{t=0} = X$. Since $c(t)$ is a curve in $\mathrm{SpSt}(2n, 2k)$, by (2.9) it must satisfy the following condition:

$$c(t)^{\mathrm{T}} J_{2n} c(t) = J_{2k}. \tag{2.10}$$

Taking the derivative of (2.10) with respect to t at $t = 0$ we get

$$\dot{c}^{\mathrm{T}}(t) J_{2n} c(t) + c^{\mathrm{T}}(t) J_{2n} \dot{c}\big|_{t=0} = X^{\mathrm{T}} J_{2n} p + p^{\mathrm{T}} J_{2n} X = 0_{2k}.$$

After moving the first term over to the left hand side, and multiplying with J_{2n} from the left, the expression simplifies to

$$p^+ X = -X^+ p.$$

We recognize this condition as $p^+ X \in \mathfrak{sp}(2k)$ as defined in (2.6). This means that for a point p,

$$T_p \mathrm{SpSt}(2n, 2k) = \left\{ X \in \mathbb{R}^{2n \times 2k} \mid p^+ X \in \mathfrak{sp}(2k) \right\}. \tag{2.11}$$

Now, after defining the symplectic Stiefel manifold, and its tangent space, we will proceed to define the righ-invariant metric on $\mathrm{SpSt}(2n, 2k)$ in preparation for defining an explicit expression of the geodesics on the manifold.

3 Right-Invariant Framework on the Symplectic Stiefel

One of the key insights of Bendokat and Zimmermann [3, p. 11] is that using a right invariant framework one is able to construct geodesics on $\mathrm{SpSt}(2n, 2k)$. Following in their footsteps, we will first define a right-invariant metric on $\mathrm{Sp}(2n)$ and its corresponding geodesics, then transport this metric to $\mathrm{SpSt}(2n, 2k)$. This will allow us to define geodesics on $\mathrm{SpSt}(2n, 2k)$. Finally, through this framework we will be able to define the Riemannian gradient, Hessian, and other tools necessary for the implementation of the optimization algorithms on the $\mathrm{SpSt}(2n, 2k)$ that we will investigate in this report.

3.1 Right-invariant metric

In this section we will define a right-invariant metric on $\mathrm{Sp}(2n)$, which will allow us to define a right-invariant metric on $\mathrm{SpSt}(2n, 2k)$. We begin by defining the point-wise right-invariant metric on $\mathrm{Sp}(2n)$ as the mapping

$$g_p^{\mathrm{Sp}} \colon T_p \mathrm{Sp}(2n) \times T_p \mathrm{Sp}(2n) \to \mathbb{R},$$
$$g_p^{\mathrm{Sp}}(X_1, X_2) \coloneqq \frac{1}{2} \mathrm{tr}((X_1 p^+)^T X_2 p^+), \quad X_1, X_2 \in T_p \mathrm{Sp}(2n). \tag{3.1}$$

We note that by "metric" we define it as in Definition 4. It is right-invariant in the sense that $g_{pq}^{\mathrm{Sp}}(X_1 q, X_2 q) = \frac{1}{2}\mathrm{tr}((X_1 q q^+ p^+)^T X_2 q q^+ p^+) = g_p^{\mathrm{Sp}}(X_1, X_2)$ for all $p \in \mathrm{Sp}(2n)$. Now that we have defined g_p^{Sp}, we want to, in a sense, transport it to $\mathrm{SpSt}(2n, 2k)$ in a way that preserves the right-invariance. To achieve this we will use a *horizontal lift* to define a metric on $\mathrm{SpSt}(2n, 2k)$ through 3.1. Split $T_p \mathrm{Sp}(2n)$ into to parts: the horizontal- and vertical part, with respect to g_p^{Sp} and π:

$$T_p \mathrm{Sp}(2n) = \mathrm{Ver}_p \mathrm{Sp}(2n) \oplus \mathrm{Hor}_p \mathrm{Sp}(2n). \tag{3.2}$$

Noting that $\mathfrak{sp}(2n) = T_I \mathrm{Sp}(2n)$, we can express these spaces through $\mathfrak{sp}(2n)$ as

$$\mathrm{Ver}_p \mathrm{Sp}(2n) \coloneqq \left\{ \Omega p \mid \Omega \in \mathrm{Ver}\, \mathfrak{sp}(2n) \right\},$$
$$\mathrm{Hor}_p \mathrm{Sp}(2n) \coloneqq \left\{ \Omega p \mid \Omega \in \mathrm{Hor}\, \mathfrak{sp}(2n) \right\},$$

where horizontal- and vertical space is defined as in Definition 7. Explicit expressions of $\mathrm{Ver}\, \mathfrak{sp}(2n)$ and $\mathrm{Hor}\, \mathfrak{sp}(2n)$ is given in [3, p. 11]. We will only need the horizontal space to define our desired geodesic, so we will only explicitly state $\mathrm{Hor}\, \mathrm{Sp}(2n)$. It is expressed as

$$\mathrm{Hor}_p \mathrm{Sp}(2n) = \left\{ \overline{\Omega} p \mid \Omega r + r\Omega - r\Omega r = \overline{\Omega} \in \mathrm{Hor}\, \mathfrak{sp}(2n) \right\},$$

where $r = J_{2n}^{\mathrm{T}}\pi(p)\pi(p)^{+}J_{2n}$. From this quotient perspective, for $p = \pi(q)$ where $q \in \mathrm{Sp}(2n)$, we can express vectors from $T_p\mathrm{SpSt}(2n, 2k)$ through $\mathrm{Hor}_p\mathrm{Sp}(2n)$. Following [11, p. 5] any $X \in T_p\mathrm{SpSt}(2n, 2k)$ and a specific $p = \pi(q)$, there exists a unique horizontal lift (see Definition 7)

$$\mathfrak{h}_q(X) = \overline{\Omega}(X)q, \tag{3.3}$$

where

$$\overline{\Omega}(X) = X(p^{\mathrm{T}}p)^{-1}p^{\mathrm{T}} + J_{2n}p(p^{\mathrm{T}}p)^{-1}X^{\mathrm{T}}\big(I_{2n} - J_{2n}^{\mathrm{T}}p(p^{\mathrm{T}}p)^{-1}p^{\mathrm{T}}J_{2n}\big)J_{2n}. \tag{3.4}$$

By [13, Thm. 2.28], we see that $\mathrm{SpSt}(2n, 2k)$ has a unique smooth manifold structure and a unique Riemannian metric such that π is a Riemannian submersion. The point-wise right-invariant Riemannian metric on $\mathrm{SpSt}(2n, 2k)$ can then be defined using (3.3) as the mapping

$$g_p \colon T_p\mathrm{SpSt}(2n, 2k) \times T_p\mathrm{SpSt}(2n, 2k) \to \mathbb{R},$$
$$g_p(X_1, X_2) \coloneqq g_p^{\mathrm{Sp}}(\mathfrak{h}_q(X_1), \mathfrak{h}_q(X_2)).$$

Expressing the mapping explicitly, we get the following expression for the right-invariant metric on $\mathrm{SpSt}(2n, 2k)$:

$$g_p(X_1, X_2) = \mathrm{tr}\left(X_1^{T}\left(I_{2n} - \frac{1}{2}J_{2n}^{T}p(p^{T}p)^{-1}p^{T}J_{2n}\right)X_2(p^{T}p)^{-1}\right), \tag{3.5}$$

for $X_1, X_2 \in T_p\mathrm{SpSt}(2n, 2k)$.

In the next section we will define an explicit expression for the geodesics on $\mathrm{SpSt}(2n, 2k)$ using the right-invariant metric we defined in this section.

3.2 Geodesics

To be able to define what it means to travel a (local) path of minimal length on any manifold, we need to define geodesics (defined generally in Definition 9). They are the generalization of straight lines in Euclidean space, and since most optimization algorithms travel along paths, they are essential in transferring Euclidean optimization algorithms to the Riemannian domain. In this section we will begin by defining geodesics on $\mathrm{Sp}(2n)$. Through the lens of quotient manifolds, and our right invariant framework, we will define geodesics on $\mathrm{SpSt}(2n, 2k)$ from the geodesics on $\mathrm{Sp}(2n)$.

Following [3, Prop. 2.1], given $p \in \mathrm{Sp}(2n)$, $X \in T_p\mathrm{Sp}(2n)$ and the right-invariant Riemannian metric (3.1), the respective geodesic $\gamma(t)$ is defined as

$$\gamma(t) \coloneqq \exp\!\big(t(Xp^{+} - (Xp^{+})^{\mathrm{T}})\big)\exp\!\big(t(Xp^{+})^{\mathrm{T}}\big)p,$$

where $\gamma(0) = p$, $\dot{\gamma}(0) = X$ and $^{+}$ is the symplectic inverse (as in (2.3)). Here, $\exp$ denotes the matrix exponential.

To be able define geodesics from the right invariant metric on $\mathrm{SpSt}(2n, 2k)$ we need the following result. According to [15, Cor. 7.46], if g_p^{SpSt} has a horizontal tangent vector at every point, it projects to a Riemannian geodesic on $\mathrm{SpSt}(2n, 2k)$.

The last preliminary definition we need is the following. In [3, Lemma 3.11] Bendokat and Zimmermann proves that if we, for a point $p \in \mathrm{Sp}(2n)$, define a geodesic $\gamma(t)$ through a horizontal tangent vector $X \in \mathrm{Hor}_p\mathrm{Sp}(2n)$, then $\dot{\gamma}(t) \in \mathrm{Hor}_{\gamma(t)}\mathrm{Sp}(2n)$. We call such a geodesic a *horizontal geodesic*.

Following [3, Prop. 3.12], we can now define a geodesic on $\mathrm{SpSt}(2n, 2k)$ through a horizontal geodesic $\gamma(t) \subseteq \mathrm{Sp}(2n)$. Let $q \in \mathrm{SpSt}(2n, 2k)$, $Y \in T_q\mathrm{SpSt}(2n, 2k)$, and $p \in \pi^{-1}(q) \subset \mathrm{Sp}(2n)$. Then the geodesic from p in direction Y is

$$\varphi(t) = \pi(\gamma(t)) = \exp\big(t(\overline{\Omega}(Y) - \overline{\Omega}(Y)^{\mathrm{T}})\big)\exp\big(t\overline{\Omega}(Y)^{\mathrm{T}}\big)p. \tag{3.6}$$

Now that we have an explicit expression for the geodesics on $\mathrm{SpSt}(2n, 2k)$, we can use them to define the Riemannian Hessian. However, one last component we need before we can express the Hessian is its predecessor: the Riemannian gradient. Therefore, in the next section we will define the Riemannian gradient on $\mathrm{SpSt}(2n, 2k)$, before moving on to the Hessian.

3.3 The Riemannian gradient

Another component to many optimization algorithms is the gradient. In the Euclidean setting the gradient of the cost function is a vector that points in the direction of the steepest ascent. Analogously, the Riemannian gradient points in the direction of the steepest ascent on the manifold. We define the notion of a Riemannian gradient rigorously in Definition 10. A useful analogy of what this means is to consider the sphere, and some cost function defining a hilly surface on the sphere. The riemannian gradient would then point in the direction towards the closest highest point, whereas the taking the negative of the riemannian gradient would point towards the closest valley floor. In this section we will state the Riemannian gradient explicitly, and prove that it satisfies necessary properties.

Proposition 1. *Given a function $f \colon \mathrm{SpSt}(2n, 2k) \to \mathbb{R}$, the Riemannian gradient (as in Definition 10) with respect to g_p is given by*

$$\mathrm{grad}\, f(p) = \nabla f(p) p^T p + J_{2n} p (\nabla f(p))^T J_{2n} p, \tag{3.7}$$

where $\nabla f(p)$ is the Euclidean gradient of a smooth extension around $p \in \mathrm{SpSt}(2n, 2k)$ in $\mathbb{R}^{2n \times 2k}$ at p.

Proof. We can see that this is the Riemannian gradient by the following two observations stated in [3, p. 12], which we verify ourselves below.

Firstly, the gradient must be in $T_p\mathrm{SpSt}(2n, 2k)$, which means by (2.11) that $0 = p^+ \mathrm{grad}\, f(p) + (\mathrm{grad}\, f(p))^+ p$. Computing this we get

$$p^{\mathrm{T}} J \nabla f(p) p^{\mathrm{T}} p + p^{\mathrm{T}} J J p (\nabla f(p))^{\mathrm{T}} J p + p^{\mathrm{T}} p (\nabla f(p))^{\mathrm{T}} J p + p^{\mathrm{T}} J^{\mathrm{T}} \nabla f(p) p^{\mathrm{T}} J^{\mathrm{T}} J p = 0,$$

where we have used $JJ = -J^{\mathrm{T}} J = -I_{2n}$ and (2.1).

Secondly, the gradient also has to satisfy $g_p(\mathrm{grad}\, f(p), X) = \mathrm{d}\, f_p(X) = \mathrm{tr}((\nabla f(p))^{\mathrm{T}} X)$ for all $X \in T_p\mathrm{SpSt}(2n, 2k)$:

$$g_p(\mathrm{grad}\, f(p), X) = \mathrm{tr}\big((p^{\mathrm{T}} p (\nabla f(p))^{\mathrm{T}} + p^{\mathrm{T}} J^{\mathrm{T}} \nabla f(p) p^{\mathrm{T}} J^{\mathrm{T}})(I_{2n} - \tfrac{1}{2} G) X (p^{\mathrm{T}} p)^{-1}\big),$$

where $G \coloneqq J^{\mathrm{T}} p (p^{\mathrm{T}} p)^{-1} p^{\mathrm{T}} J$. Expanding this expression we obtain

$$\begin{aligned}
&= \mathrm{tr}\big(p^{\mathrm{T}} p (\nabla f(p))^{\mathrm{T}} X (p^{\mathrm{T}} p)^{-1}\big) - \tfrac{1}{2} \mathrm{tr}\big(p^{\mathrm{T}} p (\nabla f(p))^{\mathrm{T}} G X (p^{\mathrm{T}} p)^{-1}\big) \\
&\quad + \mathrm{tr}\big(p^{\mathrm{T}} J^{\mathrm{T}} \nabla f(p) p^{\mathrm{T}} J^{\mathrm{T}} X (p^{\mathrm{T}} p)^{-1}\big) - \tfrac{1}{2} \mathrm{tr}\big(p^{\mathrm{T}} J^{\mathrm{T}} \nabla f(p) p^{\mathrm{T}} J^{\mathrm{T}} G X (p^{\mathrm{T}} p)^{-1}\big),
\end{aligned}$$

where the cancellations used the fact that the trace is invariant under circular shifts. Noting that the first term is by definition $\mathrm{d}\, f_p(X)$, and inserting the definition of G, the expression becomes

$$\begin{aligned}
&= \mathrm{d}\, f_p(X) - \tfrac{1}{2} \mathrm{tr}\big((\nabla f(p))^{\mathrm{T}} J^{\mathrm{T}} p (p^{\mathrm{T}} p)^{-1} p^{\mathrm{T}} J X\big) \\
&\quad + \mathrm{tr}\big(p^{\mathrm{T}} J^{\mathrm{T}} \nabla f(p) p^{\mathrm{T}} J^{\mathrm{T}} X (p^{\mathrm{T}} p)^{-1}\big) \\
&\quad - \tfrac{1}{2} \mathrm{tr}\big(p^{\mathrm{T}} J^{\mathrm{T}} \nabla f(p) p^{\mathrm{T}} J^{\mathrm{T}} J^{\mathrm{T}} p (p^{\mathrm{T}} p)^{-1} p^{\mathrm{T}} J X (p^{\mathrm{T}} p)^{-1}\big).
\end{aligned}$$

After using $J^{\mathrm{T}} J^{\mathrm{T}} = -I_{2n}$ and (2.1) on the last term, we notice that we can cancel $p^{\mathrm{T}} p (p^{\mathrm{T}}) p^{-1}$, making it equal to the second to last term. Now focusing on the second term: for the first equality we use the fact that for any matrix, A, $\mathrm{tr}(A) = \mathrm{tr}(A^{\mathrm{T}})$, and for the second equality we utilize the cyclic property of the trace, and (2.1),

$$\begin{aligned}
\tfrac{1}{2} \mathrm{tr}\big((\nabla f(p))^{\mathrm{T}} J^{\mathrm{T}} p (p^{\mathrm{T}} p)^{-1} p^{\mathrm{T}} J X\big) &= \tfrac{1}{2} \mathrm{tr}\big(X^{\mathrm{T}} J^{\mathrm{T}} p (p^{\mathrm{T}} p)^{-1} p^{\mathrm{T}} J \nabla f(p)\big) \\
&= -\tfrac{1}{2} \mathrm{tr}\big(p^{\mathrm{T}} J^{\mathrm{T}} \nabla f(p) X^{\mathrm{T}} J^{\mathrm{T}} p (p^{\mathrm{T}} p)^{-1}\big). \tag{3.8}
\end{aligned}$$

Inserting (3.8) into our expression we end up with:

$$\mathrm{d}\, f_p(X) = \mathrm{d}\, f_p(X) + \tfrac{1}{2} \mathrm{tr}\big(p^{\mathrm{T}} J \nabla f(p) X^{\mathrm{T}} J^{\mathrm{T}} p (p^{\mathrm{T}} p)^{-1}\big) + \tfrac{1}{2} \mathrm{tr}\big(p^{\mathrm{T}} J^{\mathrm{T}} \nabla f(p) p^{\mathrm{T}} J^{\mathrm{T}} X (p^{\mathrm{T}} p)^{-1}\big),$$

where the last two terms cancel after applying (2.1), and the tangent space condition (2.11), $p^{\mathrm{T}} J X = -X^{\mathrm{T}} J p$. $\qquad\square$

Now that the expression for the Riemannian gradient is established, we have almost all the tools needed to be able to define the Riemannian Hessian on $\mathrm{SpSt}(2n, 2k)$. In the next section we will define the remaining concepts, before providing an analytical expression for the Riemannian Hessian.

3.4   The Riemannian Hessian

If one knows more about the manifold, one can make more assumptions for an optimization algorithm. The hope would be that these additional assumptions would make the algorithm more efficient. In the Euclidean setting, the Hessian gives us curvature information about the cost function. Generalizing the Hessian to the Riemannian setting it gives us something similar, and we can generalize many popular algorithms. In this section we will therefore define the Riemannian Hessian of the symplectic manifold. We begin by defining what it means to take a second derivative on a manifold. After defining the necessary tools, we will give an analytical expression for the Riemannian Hessian.

Loosely following [11, Appendix A], for two smooth vector fields, $\mathcal{X}(p) = \boldsymbol{\alpha}^{\mathrm{T}} \boldsymbol{\partial}$ and $\mathcal{Y}(p) = \boldsymbol{\beta}^{\mathrm{T}} \boldsymbol{\partial}$ defined as in Definition 5, the covariant derivative (defined through the Riemannian connection by Definition 8) written in local coordinates is

$$\nabla_{\mathcal{X}} \mathcal{Y} = \sum_{i=1}^{n} \sum_{j=1}^{n} \alpha_i \partial_i(\beta_j) \partial_j + \alpha_i \beta_j \sum_{k=1}^{n} \Gamma_{ij}^k \partial_k.$$

In preparation for the Hessian, we include the description of the covariant derivative from [16, p. 96] to restrict the covariant derivative further. We want to define the covariant derivative of a vector field along a curve $c(t)$. $c(t)$ is the smooth curve, $c \colon I \to \mathcal{M}, \ t \mapsto (\gamma_1(t), \ldots, \gamma_n(t))$, where $I := [a, b] \subseteq \mathbb{R}$. Since we have an affine connection on $\mathcal{M}$, the following unique map exists:

$$\frac{D}{\mathrm{d}t} \colon \Gamma(T\mathcal{M}|_{c(t)}) \to \Gamma(T\mathcal{M}|_{c(t)}),$$

where $\Gamma(T\mathcal{M}|_{c(t)})$ denotes the the vector space of all smooth vector fields along $c(t)$. If $V \in \Gamma(T\mathcal{M}|_{c(t)})$ is induced by $\mathcal{X}$, meaning $V(t) = \mathcal{X}|_{c(t)}$, then

$$\frac{DV}{\mathrm{d}t}(t) = \nabla_{\dot{c}(t)} \mathcal{X} = \dot{\alpha}(t) + \Gamma(\alpha(t), \dot{\gamma}(t)), \quad \Gamma(u, v) = \begin{bmatrix} u^{\mathrm{T}} \Gamma^1 v \\ \vdots \\ u^{\mathrm{T}} \Gamma^n v \end{bmatrix}.$$

$\Gamma(u, v)$ is called the *Christoffel function*. If $\dot{c}(t)$ is a geodesic, the expression above reduces to

$$\ddot{\gamma}(t) = -\Gamma(\dot{\gamma}(t), \dot{\gamma}(t)), \tag{3.9}$$

since by definition geodesics must satisfy $\frac{D}{\mathrm{D}t}\dot{\gamma}(t) = 0$ and $\dot{\alpha}(t) = \dot{\gamma}(t)$. Importantly, once we have found the Christoffel symbols through (3.9), we can still use them for curves that are not geodesics. This is because the Christoffel symbols only depend on the Riemannian metric, and the local coordinates. To do this, we recover the Christoffel function for two different inputs through polarization [8, p. 312]

$$\Gamma(X, Y) = \frac{1}{4}\big(\Gamma(X + Y, X + Y) - \Gamma(X - Y, X - Y)\big),$$

where $X, Y \in \Gamma(T\mathcal{M}|_{c(t)})$.

Following [11, p. 10], to find the Christoffel symbols for $\mathrm{SpSt}(2n, 2k)$ with respect to the right invariant metric g defined in (3.5), we differentiate the geodesic formula from (3.6), and use (3.9) to achieve the following formula,

$$\Gamma(X, X) = -\ddot{\gamma}(0) = -(\overline{\Omega}(X) - \overline{\Omega}(X)^{\mathrm{T}})(X + \overline{\Omega}(X)^{\mathrm{T}} p) - (\overline{\Omega}(X)^{\mathrm{T}})^2 p.$$

Here $X = \dot{\varphi}(0) \in T_p\mathrm{SpSt}(2n, 2k)$, $p \in \mathrm{SpSt}(2n, 2k)$, and $\overline{\Omega}(X)$ is as in (3.4). With our metric g, the Hessian at p of a smooth function $f\colon \mathrm{SpSt}(2n, 2k) \to \mathbb{R}$ is the endomorphism

$$\mathrm{Hess}\, f(p)\colon T_p\mathrm{SpSt}(2n, 2k) \to T_p\mathrm{SpSt}(2n, 2k),$$

$$\mathrm{Hess}\, f(p)[X] = \frac{\mathrm{d}}{\mathrm{d}t}\, \mathrm{grad}\, f(c(t))\Big|_{t=0} + \Gamma(\mathrm{grad}\, f(p), X), \tag{3.10}$$

where $\mathrm{grad}\, f(\cdot)$ is as in (3.7). $c(t) \in \mathrm{SpSt}(2n, 2k)$ is an arbitrary curve such that $c(0) = p$ and $c'(0) = X$. Although powerful, the Hessian can become cumbersome to compute. In the next section we will give an alternative way: to compute an approximate Hessian that has the potential to be more computationally efficient.

3.5   Moving from Theory to Application

In this section, we will discuss various ways to improve the computational efficiency of the theoretical results presented above. We will first introduce the Cayley retraction, and the pseudo-Riemannian geodesic, which both approximate how we compute geodesics. Secondly we will introduce an approximate Hessian. The formulas to be optimized share a common computational challenge: they both involve computations of matrix exponentials, which are computationally expensive.

From [11, p. 7] define the *Cayley transformation* as the first-order expansion of the matrix exponential,

$$\exp(2p) \approx (I - p)(p - I)^{-1} =: \mathrm{Cay}(p).$$

Though it is only an approximation, it has the property that $\mathrm{Cay}\colon \mathfrak{sp}(2n) \to \mathrm{Sp}(2n)$. Inserting this into (3.6) gives us the *Cayley retraction* given by

$$\hat{\mathcal{R}}_p(X) = \mathrm{Cay}\left(\frac{1}{2}\big(\overline{\Omega}(X) - \overline{\Omega}(X)^{\mathrm{T}}\big)\right) \mathrm{Cay}\left(\frac{1}{2}\overline{\Omega}(X)^{\mathrm{T}}\right) p,$$

where we define the notion of retraction in Definition 12. However, we will proceed with the even simpler, yet shown to be sufficient, retraction presented in [3, p. 20]:

$$\mathcal{R}_p(tX) := \mathrm{Cay}\left(\frac{t}{2}\tilde{\Omega}(p, X)\right) p$$

$$= -p + (tq + 2p)\left(\frac{t^2}{4}q^+q - \frac{t}{2}p^+X + I\right)^{-1}, \tag{3.11}$$

where $\tilde{\Omega}(p, X) := \big(I - \frac{1}{2}pp^+\big) Xp^+ - pX^+\big(I - \frac{1}{2}pp^+\big)$, and $q := X - pp^+X$. In (3.11), the last equality comes from [3, Prop. 5.2].

Functioning as a numerical middle ground between the geodesic (3.6) on $\mathrm{SpSt}(2n, 2k)$ and the Cayley retraction (3.11), we now define the pseudo-Riemannian geodesic described in [3, p. 10]. While invoking [3] to explain the underlying theory, the pseudo-Riemannian geodesic is defined for $X \in \mathrm{SpSt}(2n, 2k)$ as

$$\phi(t) = \begin{bmatrix} p & \frac{1}{2}pr + qz \end{bmatrix} \exp\left(t \begin{bmatrix} \frac{1}{2}r & \frac{1}{2}r^2 - q^+q \\ I_{2n} & \frac{1}{2}r \end{bmatrix}\right) \begin{bmatrix} I_{2k} \\ 0 \end{bmatrix},$$

where q and r are as above.

To approximate the Riemannian Hessian defined in (3.10) we include the following approximation from [6, Corr. 5.16]. Since $\mathrm{SpSt}(2n, 2k)$ is a submanifold of a Euclidean space, then

$$\mathrm{Hess}\, f(p)[X] = \mathrm{Proj}_p(\mathrm{D}\,\overline{\mathrm{grad}}f(p)[X]), \tag{3.12}$$

where $\overline{\mathrm{grad}}f(p)$ is a smooth extension of $\mathrm{grad}\, f(p)$, and $\mathrm{Proj}_p(\cdot)$ is the projection onto the tangent space of p. The projection is defined explicitly in [11, Lemma 2.3], but we will solve it numerically through the following optimization problem. For $q \in \mathbb{R}^{2n \times 2k}$,

$$\mathrm{Proj}_p(A) \approx \min_{r \in \mathbb{R}^{2n \times 2k}} \frac{1}{2}\|r - q\|^2, \quad \text{subject to} \quad r^{\mathrm{T}}Jp + p^{\mathrm{T}}Jr = 0.$$

Having introduced the Cayley retraction, the pseudo-Riemannian geodesic, and the approximate Hessian, we have increased our toolbox in applying the theoretical results to optimization problems. The last thing on our agenda before we can conduct our experiments is to introduce the optimization algorithms we will use.

4 Algorithms

Now that we have defined the necessary theory, we can describe the algorithms of interest in this project. These algorithms use the right-invariant framework on $\mathrm{SpSt}(2n, 2k)$ to perform Riemannian optimization. By this we mean that, either through utilizing the geodesics or the Riemannian Hessian, the algorithms leverage this information to optimize some function defined on $\mathrm{SpSt}(2n, 2k)$.

In this section, we introduce the algorithms of interest in this specialization project. The algorithms we investigate are the Riemannian gradient descent algorithm, and the Riemannian trust-region method. They are used by Jensen and Zimmermann for optimization on $\mathrm{SpSt}(2n, 2k)$. One of our goals is to study the feasibility of these algorithms by attempting to reproduce some of the findings of Jensen and Zimmermann [11] as well as Bendokat and Zimmermann [3]. After introducing the two algorithms, we will outline how we implemented them, and how we conducted our experiments.

4.1 Riemannian gradient descent

The first algorithm we will define is Riemannian gradient descent (GD). Although seemingly simple, the Euclidean gradient descent (E-GD) is a powerful algorithm because of its simplicity. The lack of assumptions makes the algorithm easily applicable to a wide range of problems, and its simplicity also makes it computationally efficient. Initially following [6, p. 56], the E-GD is intuitivly transferred to the Riemannian framework. For the sequence $\{p_k\}$ where $k \in \mathbb{N}$, we have the point $p_k \in \mathrm{SpSt}(2n, 2k)$, where the next point in the sequence is computed as

$$p_{k+1} = \mathcal{R}_{p_k}(-t_k \operatorname{grad} f(p_k)).$$

Here $t_k > 0$ is some step-size to be determined.

To ensure that reach step sufficiently decreases the cost function, we will use the Riemannian version of the Armijo condition to compute t_k. In [9, p. 17] the Armijo condition for each iteration k given for $\beta \in (0, 1)$, and a search direction X_k as

$$f\big(\mathcal{R}_{p_k}(t_k X_k)\big) \leq f(p_k) + \beta t_k \langle \operatorname{grad} f(p_k), X_k \rangle_{p_k}. \tag{4.1}$$

The step-size t_k is calculated as $t_k = \gamma_k \delta^h$, where $\gamma \in (0, 1)$ is the backtracking parameter and h is the smallest integer such that (4.1) is satisfied.

Algorithm 1 Riemannian Gradient descent

Input: Initial point $p_0 \in \mathrm{SpSt}(2n, 2k)$, objective function $f \colon \mathrm{SpSt}(2n, 2k) \to \mathbb{R}$, retraction $\mathcal{R}$, parameters $\beta, \gamma \in (0, 1)$, steplength range $0 < \gamma_{\min} < \gamma_{\max}$, initial step size $\gamma_0 = f(p_0)$, maximum number of iterations $N \in \mathbb{N}$, step parameters $h_{\min} < h_{\max} \in \mathbb{Z}$, tolerance parameters $\epsilon, \epsilon_p > 0$, Riemannian metric $\langle \cdot, \cdot \rangle_p$, with Riemannian gradient $\mathrm{grad}\, f(p)$, and $||\cdot, \cdot||_{\mathrm{F}}$ denotes the Frobenius norm.

1: **for** $0 \leq k \leq N$ **do**
2:      $X_k = -\mathrm{grad}\, f(p_k)$
3:      $\gamma_k = \max(\gamma_{\min}, (\gamma_k, \gamma_{\max}))$
4:      Find t_k through solving (4.1)
5:      $p_{k+1} = \mathcal{R}_{p_k}(t_k X_k)$
6:      **if** $||\mathrm{grad}\, f(p_k)||_{\mathrm{F}} < \epsilon$ or $\frac{||p_k - p_{k+1}||_{\mathrm{F}}}{\sqrt{2n}} < \epsilon_p$ **then**
7:          Break
8:      **end if**
9: **end for**

Output: Iterates $\{p_k\}$

For robustness it is important to know if this algorithm behaves properly, in the sense that we want it to reliably converge to critical points of f. It is shown in [9, Cor. 5.8] that for $\mathrm{SpSt}(2n, 2k)$ Algorithm 1 generates an infinite sequence of iterates $\{p_k\}$[9, Prop. 5.6]. It can be shown that every accumulation point p^* of $\{p_k\}$ is a critical point of f, meaning $||\mathrm{grad}\, f(p^*)|| = 0$.

Having outlined the first order method Riemannian gradient descent, the next section will introduce the second order method Riemannian trust-region.

4.2   Riemannian trust-region method

Since the gradient descent method only uses first order information, a natural question would be to investigate how a method that utilizes second order information would perform. The criterion for this second order method to be considered better, for a specific problem, than GD would be that it, despite the (expected) increased computing time per step, would converge with few enough steps as to still beat GD.

In choosing a second order method, the simplest choice would be a Riemannian version of Newton's method (NM). Despite it's simple design, NM is known to be quite unstable, and need to be sufficiently close to a local minima to guarantee convergence [6, p. 122]. The trust-region method (TR) addresses several of the problems with NM, while still having comparatively fast convergence properties as NM locally.

Following [6, p. 131], the goal of each step k of TR is for a point p_k, is to approximate the pullback $f \circ \mathcal{R}_{p_k}(X)$ through an approximation of $T_{p_k}\mathrm{SpSt}(2n, 2k)$,

$$f(\mathcal{R}_{p_k}(X)) \approx m_{p_k}(X) = f(p_k) + \langle \mathrm{grad}\, f(p_k), X \rangle_{p_k} + \frac{1}{2}\langle H_{p_k}(X), X \rangle_{p_k}.$$

H_{p_k} can be any self-adjoint linear map on $T_{p_k}\mathrm{SpSt}(2n, 2k)$, but in our experiments H_{p_k} will be either $\mathrm{Hess}\, f(p_k)[X]$ as in (3.10), or $\mathrm{Proj}_{p_k}(\mathrm{D}\,\mathrm{grad}f(p_k)[X])$ as in (3.12). From [6, Prop. 5.44] the convergence rate of this method is essentially the same as $\mathrm{Hess}\, f(p)[X]$.

To choose a step size for TR we demand that the step must reduce the value of $m_{p_k}(X)$. Since our model is an approximation of the tangent space, we construct a trust region which is the region around p_k where we assume that the error in our approximation is negligible. We solve the TR subproblem

$$\min_{X \in T_{p_k}\mathrm{SpSt}(2n, 2k)} m_k(X) \quad \text{subject to} \quad ||X||_{p_k} \leq \Delta_k \tag{4.2}$$

to find the candidate step X_k, where candidate for next iterate then is $\hat{p}_k = \mathcal{R}_{p_k}(X_k)$. Δ_k denotes the radius of the trust region at that iterate. Depending on how the new step performs (see line

5 of Algorithm 2) it is either accepted or rejected. Finally the trust region radius is evaluated to see if it needs to be modified. The procedure is codified in Algorithm 2, which is adapted from [6, Algorithm 3.3]. To solve the subproblem in line 2 of Algorithm 2 we employ, as Jensen and Zimmermann did, the *truncated conjugate gradients method*. We will not go into more detail in this report, but further reading can be found in [6, p. 131].

Algorithm 2 Riemannian Trust-region method

Input: Initial point $p_0 \in \mathrm{SpSt}(2n, 2k)$, objective function $f \colon \mathrm{SpSt}(2n, 2k) \to \mathbb{R}$, retraction $\mathcal{R}$, maximum number of iterations $N \in \mathbb{N}$, maximal radius $\overline{\Delta} > 0$, initial radius $\Delta_0 \in (0, \overline{\Delta})$, ratio of model improvement threshold $\gamma_{\min} > 0$, tolerance parameter $\epsilon > 0$, Riemannian metric $\langle \cdot, \cdot \rangle_p$, with Riemannian gradient $\mathrm{grad}\, f(p)$, and $||\cdot, \cdot||_{\mathrm{F}}$ denotes the Frobenius norm.

1: **for** $0 \leq k \leq N$ **do**
2:      Find X_k through solving (4.2)
3:      $\hat{p} = \mathcal{R}_{p_k}(X_k)$
4:      $\gamma_k = \big(f(p_k) - f(\hat{p})\big) / \big(m_k(0) - m_k(X_k)\big)$
5:      Compute new iterate
$$p_{k+1} = \begin{cases} \hat{p} & \text{if } \gamma_k > \gamma_{\min} \\ p_k & \text{otherwise} \end{cases}$$

6:      Compute new trust-region radius

$$\Delta_{k+1} = \begin{cases} \frac{1}{4}\Delta_k & \text{if } \gamma_k < \frac{1}{4} \\ \min\left\{2\Delta_k, \overline{\Delta}_k\right\} & \text{if } \gamma > \frac{3}{4} \text{ and } ||X_k|| = \Delta_k \\ \Delta_k & \text{otherwise} \end{cases}$$

7:      **if** $||\mathrm{grad}\, f(p_k)||_{\mathrm{F}} < \epsilon$ **then**
8:          Break
9:      **end if**
10: **end for**
Output: Iterates $\{p_k\}$

Convergence and stability of TR is presented in-depth in [6, p. 147]. However, for consistency we note here that given sufficient assumptions (which are met in our examples), by [6, Cor. 6.24] for $\{p_k\}$ generated by TR,
$$\liminf_{k \to \infty} ||\mathrm{grad}\, f(p_k)||_{p_k} = 0.$$

In other words, this means that for all $\epsilon > 0$ and K there exists $k \geq K$ such that $||\mathrm{grad}\, f(p_k)||_{p_k} \leq \epsilon$.

Now that we have defined the Riemannian counterparts for GD and TR, we have all of the tools necessary to conduct our experiments. In the next section we will discuss some minor details around the implementation before moving on to the actual experiments.

4.3 Implementation

In this section we will outline how we will conduct our experiments. We will first define which retractions and algorithms we will test, as well as presenting the main packages we will use to implement the experiments. Finally we will cite where one can find the code used in the following experiments.

Before comparing algorithms, we will first look at the feasibility off the different retractions defined in section 3.5. These are the Cayley retraction, the pseudo-Riemannian geodesic, and the Riemannian geodesic. The motivation for this experiment is to test how the different retractions perform in terms of speed and accuracy, with the goal of finding which retraction to use in the subsequent experiments.

We will use three algorithms for our experiments. The first is the gradient descent algorithm using

the Armijo condition to find appropriate step sizes, denoted as GD. The second is the trust-region algorithm using the exact Riemannian Hessian Hess $f(p_k)[X]$ as in (3.10), denoted as TR-1. The final algorithm, which we will denote as TR-2, will differ from TR-1 by using the approximate Hessian $\text{Proj}_{p_k}(\text{D}\,\overline{\text{grad}}f(p_k)[X])$ defined in (3.12). The shorthand TR will be used when reffering to both TR-1 and TR-2.

The code for the experiments are mainly using the two packages Manifolds.jl [2] and Manopt.jl [4]. Manifolds.jl provides us with a useful framework to be able to work with their implementation of the symplectic Stiefel manifold. Manopt.jl provides us with a high level framework to be able to implement the optimization algorithms. An effort has been made to ensure the parameters in functions and objects defined in the utilized libraries are consistent as to align with the theory presented in this project report.

All files used to produce the data in this report are available in the following github repository [10].

5   Numerical Experiments

In this section we present the numerical experiments, and results, conducted in this report. We have conducted the following three experiments:

1. retraction comparison through the nearest symplectic matrix problem using GD,

2. comparing the performance of GD, TR-1, and TR-2 through the nearest symplectic matrix problem, and

3. comparing the GD, TR-1, and TR-2 through the problem of performing a proper symplectic decomposition.

The problem of nearest symplectic matrix is used in both Bendokat and Zimmermann [3, p. 25] as well as Jensen and Zimmermann [11, p. 15], and the problem of proper symplectic decomposition is used in Jensen and Zimmermann [11, p. 17]. The first experiment is conducted in a similar manner to Bendokat and Zimmermann [3, p. 25], where we leverage the problem of nearest symplectic matrix to compare the performance of the Cayley retraction, the Riemannian geodesic, and the pseudo-Riemannian geodesic through the use of GD. The second and third experiments are conducted similarly to the analogous experiments in Jensen and Zimmermann [11, p. 15 & 17] where the purpose of these two experiments is to compare the performance of the GD, TR-1 and TR-2 algorithms. The reason for conducting both of these experiments is to make the conclusions we derive more robust than if only one experiment was conducted.

The experiments are performed using Julia version 1.10.2 on the Laptop ACER Swift SF314-43 processor AMD Ryzen 7 5700U with Radeon Graphics 1.80GHz and 16GB of RAM. To ensure reproducibility, all of the random processes are seeded using the seed 42. For readability, the code is written in the Pluto.jl notebook format, a format that allows for interactive code execution and visualization in a similar manner to the Python equivalent "Jupyter notebook".

5.1   Nearest Symplectic Matrix Problem - Retraction comparison

Before we compare GD and TR, we will verify the performance of the Cayley retraction, Riemannian geodesics, and pseudo-Riemannian geodesics on $\text{SpSt}(2n, 2k)$. To test and compare the feasibility of our retractions we will, similarly to [3, p. 25], try to solve the following problem called the *nearest symplectic matrix problem*. For a matrix $q \in \mathbb{R}^{2n \times 2k}$ we want to find the closest symplectic matrix $p \in \text{SpSt}(2n, 2k)$. We formalize this in as the following optimization problem,

$$\min_{p \in \text{SpSt}(2n,2k)} f(p), \quad \text{where} \quad f(p) := \tfrac{1}{2}||q - p||_{\text{F}}^2. \tag{5.1}$$
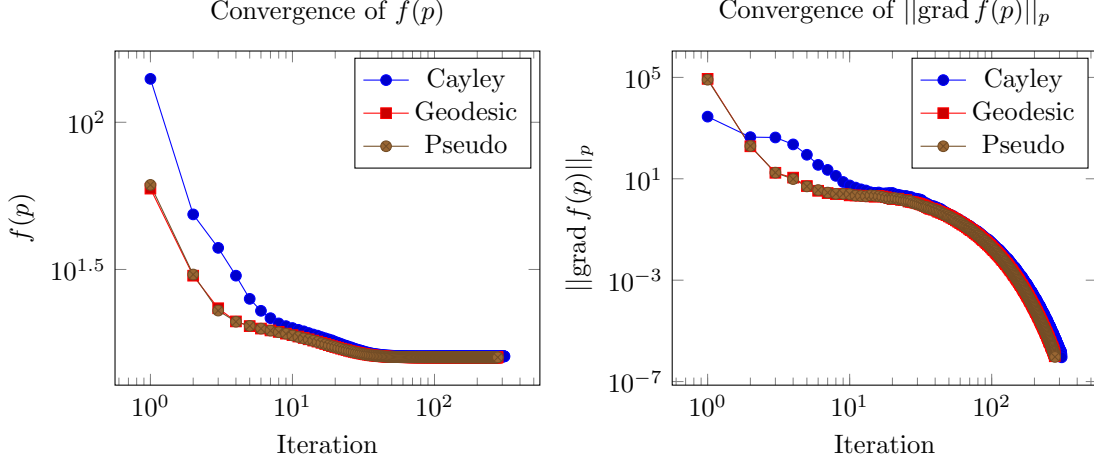
Figure 1: Nearest symplectic matrix problem solved by GD for different retractions. The figure displays the value of $f(p)$ and $||\text{grad}\, f(p)||_p$ on $\text{SpSt}(2n, 2k)$ as a function of iteration using Cayley retraction, Riemannian geodesics, and pseudo-Riemannian geodesics, with $n = 1000$ for $k = 20$.

Table 1: Nearest symplectic matrix problem solved by GD for different retractions. The table summarizes time to converge using Cayley retraction, Riemannian geodesics, and pseudo-Riemannian geodesics on $\text{SpSt}(2n, 2k)$, with $n = 1000$ for $k = \{5, 10, 20\}$.

	Runtime (s)		
	Cayley	Geodesic	Pseudo
$k = 5$	0.52	0.73	0.49
$k = 10$	1.6	2.8	1.7
$k = 20$	5.4	7.9	5.0

For a point $p \in \text{SpSt}(2n, 2k)$ and $X \in T_p\text{SpSt}(2n, 2k)$, Euclidean gradient and Hessian of $f(p)$ are, respectively,

$$\nabla f(p) = p - q, \quad \nabla^2 f(p)[X] = X.$$

For the experiments we generate q randomly, and normalize it, $q \cdot ||q||_{\text{F}}^{-1}$. For the optimization runs we choose $n = 1000$ and $k = \{10, 50, 100\}$. The results is displayed in Table 1 and in Figure 1.

In Figure 1 we chose only to plot the optimization run for $n = 1000$, $k = 20$ since the other runs followed a similar pattern. We observe in the figure that the Riemannian Geodesic and the pseudo-Riemannian geodesic performed similarly in the sense that the pseudo-Riemannian geodesic did not drift away far from the Riemannian Geodesic in either the value for $f(p)$ nor $||\text{grad}\, f(p)||_p$. Cayley, on the other hand, is less accurate in the first ~ 10 iterations than the other two in both $f(p)$ and $||\text{grad}\, f(p)||_p$. Despite this, it quickly caches up to the others, and converges in a comparable amount of steps.

Regarding Table 1 we can see a clear pattern of all three using using more time to converge as we increase the dimension k. We observe that the Riemannian geodesic performs somewhat worse than the other two for all three runs. Interestingly, the Cayley retraction and the pseudo-Riemannian geodesic performed almost identically, in terms of wall-clock speed, in all three runs.

Despite the promising results of the pseudo-Riemannian geodesic, we will not use it in the following experiments, rather we will use the Cayley retraction. The reason for this is twofold. The first reason is that the Cayley retraction is already implemented in Manopt.jl. This means that it has been tested and verified to work by numerous users, and developers, and is therefore probably more reliable. The second reason is that in an experiment in [3, p. 26] they found both the Riemannian geodesic and the pseudo-Riemannian geodesic to be exponentially more inaccurate for large stepsizes. Because of these two reasons, in an effort to make the experiments more independent, we will proceed with using the Manopt.jl implementation of the Cayley retraction.

Table 2: Nearest symplectic matrix problem solved by GD, TR-1 and TR-2. The table summarizes time to converge for all the algorithms on $\mathrm{SpSt}(2n, 2k)$, with $n = 100$ for $k = 5, 10, 20$.

	Runtime (s)		
	GD	TR-1	TR-2
$k = 5$	0.051	9.7	0.70
$k = 10$	0.23	12	5.4
$k = 20$	1.1	35	23

5.2 Nearest Symplectic Matrix Problem - 2nd Order

As in the preceding section, we will conduct our experiments on the optimization problem called the nearest symplectic matrix problem, (5.1). Striving to replicate the conditions in [11, p. 15], for $\mathrm{SpSt}(2n, 2k)$ we select $n = 100$, and $k = \{5, 10, 20\}$. The algorithms tested are GD, TR-1 and TR-2. The results of these runs are summarized in Table 2 and Figure 2.

Figure 2 shows $f(p)$ and $||\mathrm{grad}\, f(p)||_p$ as a function of iteration for the three different runs with $k = \{5, 10, 20\}$, for the three algorithms GD, TR-1 and TR-2. We observe that for all ks, the algorithms behaved similarly in the sense that they all converged in a similar number of steps, and following a similar shape. We observe that TR-1 and TR-2 behaves similarly, so we will denote both of them as TR. The only major pattern to be observed between k's is that the first ~ 15 iterations of TR in $k = 5$ have a steeper slope than GD. This difference is smaller for $k = 10$, and almost non-existent in $k = 20$. Looking at $||\mathrm{grad}\, f(p)||_p$ we observe that the major difference in convergence, as theoretically predicted, is visible after the first ~ 15 iterations. after this point, while the convergence rate of GD seem to slow down, the convergence rate of TR seems to increase. It should be noted that this "speeding up" and "slowing down" is an artifact of the loglog plotting, but it is clearly showing that the rate of convergence close to the critical point is fundamentally different between TR and GD. It should also be noted that all algorithms terminated as the result of hitting the condition $||\mathrm{grad}\, f(p)||_p \leq 10^{-6}$. This can give the perception that the final iteration of TR is more precise than GD. However, this is only an artefact of the convergence rate of TR being so high that the final step before convergence is detected, significantly overshoots the convergence condition for $k = \{5, 10\}$.

Table 2 displays the time to converge for the runs displayed in Figure 2. We can see that GD has a significantly faster time to converge than TR-1 and TR-2. We also observe that TR-2 is faster than TR-1, though the difference in time shrinks as k increases. We can also see that the time increase per k for TR-1 and TR-2 is much slower than for GD, which increases the convergence time by approximately an order of magnitude for the increases in k.

5.3 The Proper Symplectic Decomposition Problem

The final experiment we will conduct is to apply GD, TR-1 and TR-2 to the problem of computing the proper symplectic decomposition of a matrix $s \in \mathbb{R}^{2n \times 2m}$ in a similar manner to Jensen and Zimmermann [11, p. 18]. This problem is an important task in symplectic model order reduction of Hamiltonian systems. This problem can be formulated as the following optimization problem:

$$\min_{p \in \mathrm{SpSt}(2n, 2k)} f(p), \quad \text{where} \quad f(p) := ||s - pp^+ s||_{\mathrm{F}}^2. \tag{5.2}$$

In most applications $k \ll n$. For a point $p \in \mathrm{SpSt}(2n, 2k)$ and $X \in T_p\mathrm{SpSt}(2n, 2k)$, Euclidean gradient and Hessian are, respectively,

$$\nabla f(p) = -2\big((I - pp^+)ss^{\mathrm{T}}J^{\mathrm{T}}pJ - Jss^{\mathrm{T}}(I - pp^+)^{\mathrm{T}}pJ\big),$$
$$\nabla^2 f(p)[X] = -2(\alpha(p, X)pJ + \eta XJ - \alpha(p, X)^{\mathrm{T}}pJ - \eta^{\mathrm{T}}XJ),$$

where $\alpha(p, X) = \beta(p, X)ss^{\mathrm{T}}J$ where $\beta(p, X) = \mathrm{D}(I - pp^+)[X] = -Xp^+ - (Xp^+)^+$, and $\eta = (I - pp^+)SS^{\mathrm{T}}J^{\mathrm{T}}$. To construct s, we generate a matrix $u \in \mathrm{SpSt}(2n, 2r)$ as well as another matrix
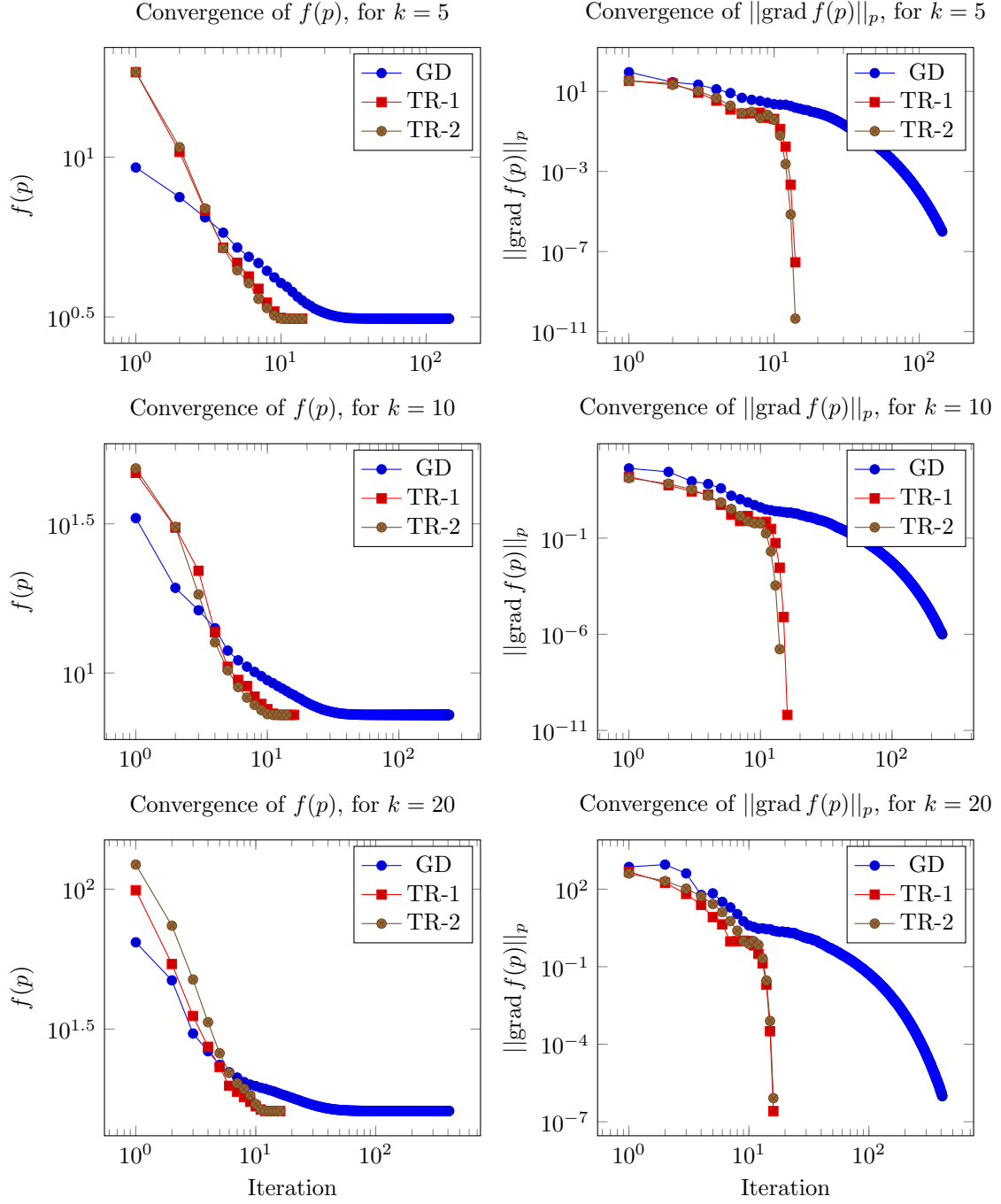
Figure 2: Nearest symplectic matrix problem solved by GD, TR-1 and TR-2. The figures show $f(p)$ and $||\text{grad } f(p)||_p$ on $\text{SpSt}(2n, 2k)$ as a function of iteration for all three algorithms, with $n = 100$ for $k = 5, 10, 20$.
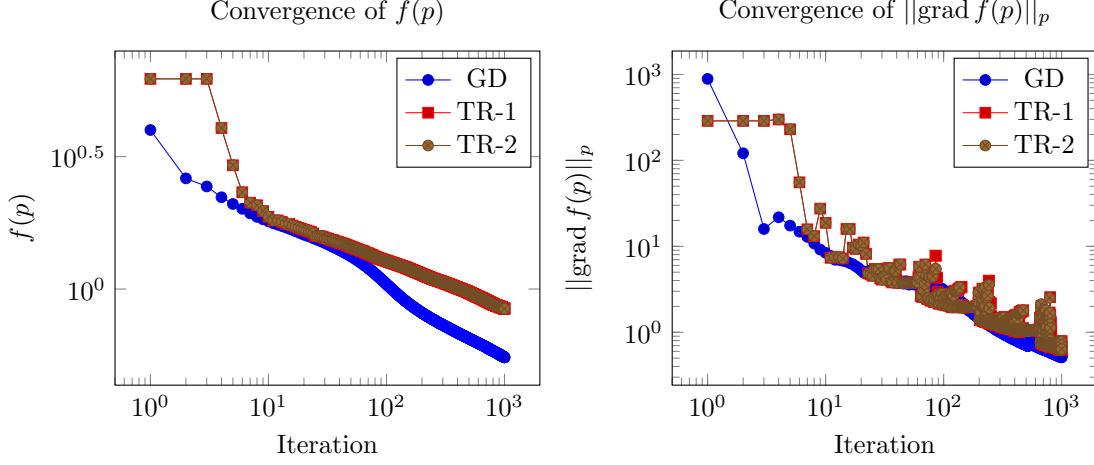
Figure 3: The proper symplectic decomposition problem attempted solved by GD, TR-1 and TR-2 on $\mathrm{SpSt}(2n, 2k)$, with $n = 100$, $k = 10$, $r = 20$, and $m = 30$. None of the algorithms converged.

$v \in \mathbb{R}^{2r \times 2m}$, which we normalize; $v = v \cdot ||v||_{\mathrm{F}}^{-1}$. From these two matrices we generate $s = u \cdot v$. For the optimization run we choose $n = 100$, $k = 10$, $r = 20$, and $m = 30$. The results are displayed in Figure 3.

It is clear from Figure 3 that none of the algorithms converge as expected from the theory. We observe that all three algorithms are stopped by the maximum iteration count set at 10^3 iterations. In addition, all three algorithms follow the pattern of very low convergence rate. The last thing all three algorithms share, is that they all have some temporary increase in the value of $||\mathrm{grad}\, f(p)||_p$. This is not infeasible for TR-1 and TR-2, but quite odd for GD. Similarly to Figure 2, the values of TR-1 and TR-2 have, for both $f(p)$ and $||\mathrm{grad}\, f(p)||_p$, almost the same function value for all steps.

6   Conclusion

In this report we presented the right-invariant framework on the symplectic Stiefel manifold. Through this framework we presented the Riemannian gradient descent algorithm (GD) and the Riemannian trust-region method using the exact Riemannian Hessian (TR-1) and the approximate Riemannian Hessian (TR-2). We used GD to analyze the performance of the Cayley retraction, the pseudo-Riemannian geodesic retraction, and the Riemannian geodesic retraction on the problem of finding the nearest symplectic matrix. Lastly we used the same problem, as well as the proper symplectic decomposition problem, to compare the three algorithms.

Regarding the retraction experiment, in section 5.1, apart from reaffirming the dominance of the Cayley retraction over the Riemannian geodesic in terms of computational efficiency (as observed in both [11, p. 8] and [3, p. 26]), we also found that the pseudo-Riemannian geodesic performed comparably or better than the Cayley retraction. It is unexpected that the pseudo-Riemannian geodesic performed as well as it did seeing as in [3, p. 28] it was excluded from a similar test to the one presented in this report. This was because it seemed to do rather unimpressively in an earlier test Bendokat and Zimmermann performed. Given that the pseudo-Riemannian geodesic was seemingly as accurate as the Riemannian geodesic, in addition to being as fast as the Cayley transformation, further investigation into the pseudo-Riemannian geodesic is warranted.

Regarding using the nearest symplectic matrix problem to compare GD, TR-1, and TR-2, the results for the experiments presented in Section 5.2 are in line with the experiment done by Jensen and Zimmermann [11, Tbl. 4.1]. We observed on $\mathrm{SpSt}(2n, 2k)$ for $n = 100$, and $k = \{5, 10, 20\}$ that GD was superior in terms of runtime, with indication that this might not be the case for larger problems. This is indeed what Jensen and Zimmermann observes for $n = 1000$, and $k = \{10, 50, 100\}$, with GD slightly beating the others for $k = 10$, and ultimately TR-2 surpassing GD

in terms of speed for $k = \{50, 100\}$. It should be noted that Jensen and Zimmermann used a more costly retraction [11, Fig. 1] than what we used. Despite this the results for GD we observed are not in conflict with other experiments either like in [3, Tbl. 1]. Another point worth noting is that the superior numerical accuracy by TR-1 and TR-2 pointed out by Jensen and Zimmermann, which they conclude is purely due to the fact that TR-1 and TR-2 make use of second order information, could be misinterpreted. As we commented on in section 5.2, we can see in Figure 2 that TR-1 and TR-2 tend to overshoot the convergence condition of $\|\text{grad}\, f(p)\|_p \leq 10^{-6}$, while GD does not. This effect has the potential to muddy the waters when comparing accuracies of TR-1 and TR-2 to GD. Despite this concern, we do observe that for larger systems, i.e. larger k, this effect became smaller. It is therefore possible that for the larger system Jensen and Zimmermann tested, the overshooting effect was negligible.

For the problem of performing a proper symplectic decomposition using GD, TR-1 and TR-2, as done in Section 5.3, the code for the nearest symplectic element experiment and the proper symplectic decomposition is nearly identical - but for the optimization problem itself. Despite this, while in the nearest symplectic matrix problem all algorithms converge, none of them do in this experiment. Since Jensen and Zimmermann published their code on github [11, p. 15], we were able to compare their MATLAB code with our Julia code. After generating matrices for p, s, and X in Julia, we inserted these into the MATLAB code. Through this we were able to verify that $f(p)$, $\nabla f(p)$, and $\nabla^2 f(p)[X]$ output equivalent matrices in both frameworks. The fact that all three are failing to converge could be because grad $f(p)$ is not correct. However, Manopt.jl's built-in functions "checkgradient" as well as "checkhessian" shows that both the Riemannian gradient, as well as the Hessian, look correct. In fact, as MATLAB's manopt also has a "checkgradient"-function, inserting the same p and X as in Julia gives almost the exact same result. These debugging results lead us to conclude that either we were unlucky with our starting point or s, or there is some problem with the rest of the code that is not of consequence in the nearest symplectic element experiment. Of the two alternatives the second one seems more likely. As the implementation of GD and TR used in our experiments were the ones already implemented in manopt.jl, there might be some additional condition that one needs to change for them to be comparable to the implementations in MATLAB. Since this problem has been rigorously narrowed down in our code, further investigations into solutions may be warranted.

It should be noted that since the testes were performed on a laptop, there is a high degree of uncertainty in all of the timed runs. This is because, like most laptops, when they heat up above a certain temperature, the processor will throttle down to prevent overheating. This results in the operations taking longer time, and the comparison between different runs becomes less reliable. Running the tests on a setup with a more stable temperature would likely produce more reliable results.

Bibliography

[1] P.-A. Absil, R Mahony and R Sepulchre. *Optimization Algorithms on Matrix Manifolds*. Princeton University Press, 2008. ISBN: 9780691132983.

[2] Seth D. Axen et al. 'Manifolds.Jl: An Extensible Julia Framework for Data Analysis on Manifolds'. In: *ACM Transactions on Mathematical Software* 49.4 (Dec. 2023). DOI: 10.1145/3618296.

[3] Thomas Bendokat and Ralf Zimmermann. *The real symplectic Stiefel and Grassmann manifolds: metrics, geodesics and applications*. 2021. arXiv: arXiv:2108.12447v1.

[4] Ronny Bergmann. 'Manopt.jl: Optimization on Manifolds in Julia'. In: *Journal of Open Source Software* 7.70 (2022), p. 3866. DOI: 10.21105/joss.03866.

[5] William M. Boothby. *An Introduction to Differentiable Manifolds and Riemannian Geometry*. Vol. 63. Elsevier Science (USA), 1975. DOI: https://doi.org/10.1016/S0079-8169(08)61028-4.

[6] Nicolas Boumal. *An introduction to optimization on smooth manifolds*. Cambridge University Press, 2023. DOI: 10.1017/9781009166164. URL: https://www.nicolasboumal.net/book.

[7] Henri Bourles. *Fundamentals of Advanced Mathematics V3*. Elsevier Ltd., 2019. DOI: 10.1016/c2017-0-00728-0.

[8] Alan Edelman, Tomás A. Arias and Steven T. Smith. 'The Geometry of Algorithms with Orthogonality Constraints'. In: *SIAM Journal on Matrix Analysis and Applications* 20 (1998). DOI: 10.1137/s0895479895290954. arXiv: arXiv:physics/9806030v1.

[9] Bin Gao et al. 'Riemannian optimization on the symplectic Stiefel manifold'. In: *SIAM Journal on Optimization* 31 (2021). DOI: https://doi.org/10.1137/20M1348522. arXiv: arXiv:2006.15226.

[10] Ole Gunnar Røsholt Hovland. *TMA4500-Project-Hovland-Symplectic-Stiefel*. 2024. URL: https://github.com/kellertuer/TMA4500-Project-Hovland-Symplectic-Stiefel.git.

[11] Rasmus Jensen and Ralf Zimmermann. *Riemannian optimization on the symplectic Stiefel manifold using second-order information*. 2024. arXiv: arXiv:2404.08463v2.

[12] Jon Arnt Kårstad. *Template Project NTNU*. URL: https://no.overleaf.com/latex/templates/template-project-ntnu/zjystqvqztpg (visited on 11th Sept. 2024).

[13] John M. Lee. *Introduction to Riemannian Manifolds*. 2nd ed. Springer Cham, 2018. DOI: 10.1007/978-3-319-91755-9.

[14] John M. Lee. *Introduction to Smooth Manifolds*. 2nd ed. Springer New York, NY, 2012. DOI: 10.1007/978-1-4419-9982-5.

[15] Barett O'Neill. *Semi-Riemannian Geometry With Applications to Relativity*. Vol. 103. Academic Press, 1983. ISBN: 9780125267403.

[16] Loring W. Tu. *Differential Geometry*. Springer International Publishing, 2017. DOI: 10.1007/978-3-319-55084-8.